HOKKAIDO UNIVERSITY

Title	Seismic response of highway viaducts equipped with lead-rubber bearings under low temperature
Author(s)	Deng, Pengru; Gan, Zhiping; Hayashikawa, Toshiro; Matsumoto, Takashi
Citation	Engineering structures, 209, 110008 https://doi.org/10.1016/j.engstruct.2019.110008
Issue Date	2020-04-15
Doc URL	http://hdl.handle.net/2115/84428
Rights	© <2019>. This manuscript version is made available under the CC-BY-NC-ND 4.0 license https://creativecommons.org/licenses/by-nc-nd/4.0/
Rights(URL)	https://creativecommons.org/licenses/by-nc-nd/4.0/
Type	article (author version)
File Information	20200430_Manuscript For HUSCAP.pdf

Seismic Response of Highway Viaducts Equipped with Lead-Rubber Bearings under Low

Temperature

Pengru Deng[1], Zhiping Gan[2*], Toshiro Hayashikawa[3], Takashi Matsumoto[4]

[1] Assistant Professor, Faculty of Engineering, Hokkaido University, Hokkaido 060-8628, Japan; Email: pengrudeng@eng.hokudai.ac.jp
[2*]Daiwa Lease Corporation Limited, Tokyo 102-0072, Japan; Email: zpgan1024@gmail.com (Corresponding author)
[3] Emeritus Professor, Faculty of Engineering, Hokkaido University, Hokkaido 060-8628, Japan; Email: toshiroh@eng.hokudai.ac.jp
[4] Professor, Faculty of Engineering, Hokkaido University, Hokkaido 060-8628, Japan; Email: takashim@eng.kokudai.ac.jp

ABSTRACT

Based on a FEM based nonlinear dynamic numerical method, this study investigates the detrimental effects of low temperature on the seismic responses of a highway viaduct equipped with Lead-Rubber Bearings (LRBs). In this method, a dynamic bearing property definition is introduced to account for the temperature variation caused by the absorbed earthquake energy and the corresponding property variation of LRBs. Under low temperature conditions, the base isolation effect of LRBs which are well-designed for room temperature is significantly weakened, manifested by shorter fundamental structural natural periods and more damages and forces imposed to structure members, such as a 5-13% increment of shear force transferred by the LRBs, an increasing area of the hysteresis loop of the bending moment at the bottom of piers, and an increasing residual displacement at the top of piers. In addition, through jointed investigating the seismic responses under both long and short durations of earthquake motions, it is demonstrated that the heat production in LRBs over an earthquake can alleviate the detrimental effect of low temperature, and the extent of this alleviation is positively correlated to the earthquake duration. Therefore, the low temperature effect and the property variation of LRBs over an earthquake should be comprehensively considered for the designation of LRBs installed in bridge viaducts located in cold regions and the realization of an accurate seismic analysis of the bridge viaducts.

KEYWORDS

LRB; Bridge; Low temperature; Seismic isolation; Nonlinear dynamic analysis

1 INTRODUCTION

In modern transportation networks, highway viaducts especially curved viaducts are extensively employed taking advantage of their strong capability on circumventing geometric restrictions and constraints of limited site space [1-3]. Additionally, the curved alignments offer the benefits of aesthetically pleasures, good traffic sight, and economically competitive construction costs with regard to straight bridges. Unfortunately, such essential structures are more vulnerable to earthquakes than the standard straight viaducts because of the coupling of in-plane and out-plane bending and torsional forces or deformations. This easily vulnerable characteristic has been revealed by post-earthquake surveys where tremendous

economic losses and serious social inconveniences were found due to a collapse or even non-collapsed damage of highway viaducts [4, 5]. Therefore, it is of great significance to improve the earthquake resistance of highway viaducts to ensure their safety and functionality after severe earthquakes.

For eliminating earthquake-induced damages on bridges, one of the most effective and efficient approaches is setting an isolation system between the superstructures and their supporting substructures [6, 7]. Conceptually, seismic isolation systems should decouple the bridge superstructures from the horizontal components of ground motions. Hence, an isolation system is generally designed with strong flexibility which cuts down the forces transferred from substructures to superstructures. Meanwhile, this flexibility shifts the fundamental frequencies of a bridge away from the dominant frequencies of earthquakes. In addition, the isolation system provides an additional means of energy dissipating, thereby reducing the damaging energy exerted on the bridge piers.

In the last few decades, researchers have developed and tested a series of seismic isolation devices where a lead-rubber bearing (LRB) exhibited extreme good working performances and wide applicability [8, 9] owing to its simplicity and combined isolation-energy dissipation function in a single compact unit. These bearings are multilayered, laminated elastomeric bearings that are formed by bonding sheets of rubber to thin steel reinforcing plates with one or more circular holes. Lead plugs are inserted into these holes. On one hand, the LRB is very stiff and strong in the vertical direction because the internal steel reinforcing plates afford the vertical load capacity. As a result, the LRBs behave like regular bearings under normal conditions. On the other hand, as the elastomeric rubber affords the isolation component with lateral flexibility and the lead cores affords the energy dissipation [10, 11], the LRBs can not only absorb seismic energy during a strong earthquake event but also provide rigidity against earthquakes, wind, and service loads [12-14].

According to the above introduction, the LRB is mainly made of rubber. Thus, the serviceability of LRBs depends on the embedded rubber which has temperature dependent behaviors due to its material characteristics as an elastomer type of polymer. The rubber translates from an elastomeric, rubbery phase to a brittle, glassy solid amorphous phase with respect to a decreasing temperature. Correspondingly, the stiffness of rubber increases [15, 16]. Based on experimental results, it is found that the equivalent stiffness of LRB increases about 30% due to a long-term low temperature accumulation. With the increment of the stiffness of rubber material, the flexibility of base isolation devices is deteriorated and thereby its seismic protecting capability is weakened [17]. In addition, cold regions where snow and ice occur at least part of the year account for a large proportion of the world's land [18]. However, the temperature of the LRBs may increases with respect of time during a strong earthquake because the lead plugs of LRBs can absorb seismic energy and release it as heat [10, 11]. Therefore, the temperature related performance of base isolation devices should be investigated and uncovered, which is still a field lacking comprehensive understanding after years of researches.

This study aims at investigating and generalizing the effects of low temperature on the seismic responses of a curved highway viaduct equipped with LRBs, which is an extensively employed structural system in the cold Hokkaido Island of Japan, through conducting nonlinear dynamic analyses on the bridges under room and low temperature conditions. Considering a temperature variation in LRBs due to the absorbed earthquake energy, a dynamic property definition for LRBs is introduced and both fixed low and dynamic low temperature conditions are employed. The obtained results indicate that the base isolation effect of LRBs is significantly weakened due to the low temperature, and consequently more forces and damages are imposed to structural members. In addition, the necessities of including the dynamic property definition for an accurate seismic analysis is emphasized by the seismic responses of the viaduct subjected to short and long durations of earthquake motions. Finally, the study proposes some recommendations for seismic design and analysis of curved highway viaducts equipped with LRBs and located in cold regions.

2 ANALYTICAL MODEL OF VIADUCTS

For curved highway viaducts, on one hand, an earthquake may lead to complex vibration movements along different directions. It has been repeatedly demonstrated that during a strong earthquake, adjacent spans often vibrate out-of-phase, causing three main types of movement related problems, i.e. deck superstructure unseating, adjacent spans pounding together at the joints, and fragile of the connection between deck superstructure and substructure members. Thus, one should at least exploit a three-dimensional model for a realistic prediction of the highway viaducts seismic responses. On the other hand, damages to structural members are acceptable in current design philosophies under strong earthquakes which may generate extreme ground motions and cause near-fault damages. Correspondingly, the employed model for piers and bearings should include the geometrical and material nonlinearities to account for the possible post-elastic material behaviors and large structural deformations, respectively. Therefore, the present study employs a 3D nonlinear modeling of the entire highway viaducts system. The bridge piers and bearing supports are modeled with nonlinear 3D fiber elements, whereas the superstructure is represented by a planar grillage beam system. As a result, the responses of the viaducts induced by the joint effects of longitudinal, transverse, and vertical earthquake excitations can be evaluated with the 3D analytical model. In addition, this 3D analytical model provides a tool of investigating the material and geometric nonlinearities related nonlinear behaviors under severe earthquakes.

2.1 Superstructure and piers

The present study analyzes a typical three-span continuous curved highway viaduct which may locate among a series of viaducts. Hence, on abutment is accounted for in analyses. The continuous superstructures are supported by the bearing system rested on the top of box-sectional steel bridge piers which are widely used to support highway viaducts in urban areas, being considered advantageous in regions of high seismic activity [19, 20].

The overall viaduct length of 120 m is divided equally into three spans of 40 m. The bridge alignment is horizontally curved in a circular arc with a curvature of 100 m. The curvature is measured from the origin of the circular arc to the center-line of the deck superstructure. The global coordinate system for the viaduct is also shown in **Figure 1**, where the global X- and Y-axes lie in the horizontal plane whereas the global Z-axis is along vertical direction. The steel box which has a 0.8 m^2 of sectional area is employed for the girder superstructure as shown in **Figure 2**. With respect to the sectional local y- and z- axes (**Figure 1(a)**), the cross sectional moment of inertia are simply calculated equaling 0.355 m^4 and 1.519 m^4, respectively. And the torsional constant is 4.018 m^4. To facilitate structural modeling, the superstructure is modelled as an equivalent box cross section which has the approximate same sectional area and moments of inertia as the actual steel box girder cross section. Given that the density of steel and concrete is 7850 and 2500 kg/m^3 respectively, the total weight of the superstructure is calculated equaling 8.82 MN.

As for the steel bridge piers, a four thin-walled hollow box section which is designed following the seismic coefficient method given in the Specifications for Highway Bridges in Japan [21] is employed for the viaduct. All the piers have the same height of 20 m. This hollow box-section is commonly used in steel bridge piers in Japan because it possesses high strength/mass ratios and significant ductility, which dramatically enhance its structural performance during strong earthquakes.

In this analysis, superstructure components are modelled by the nonlinear space beam elements. As for the pier members, a fiber element modelization (**Figure 3**) which is accepted as an accurate and practical technique for computing the responses of structural members is used to simulate the characterizations of

them. In the fiber element model, the elemental cross-section is subdivided into a discrete number of longitudinal and transversal small regions (fibers). For every fiber, its constitutive model is based on the material uniaxial stress-strain relation. With the discretization along both directions and actual material stress-strain relations including plasticity, the inelasticity of flexural members can be accounted for in the fiber element model. From analysis, one can obtain the stresses in each fiber zone which are then exploited in determining the element stress resultants through integrating them over the cross section of the element. In this study, the steel stress-strain relation is represented by a bilinear nonlinear model with the yielding strength, Young's modulus, and the strain hardening in plastic area equaling 235.4 MPa, 200 GPa, and 0.01, respectively.

2.2   Lead-rubber bearings (LRBs)

The viaduct superstructures are supported on lead rubber bearings (LRBs) which rest on the top of all piers. Even though the LRBs can absorb seismic energy and abate the seismic energy or damage imposed on superstructures owing to their flexibility, this strong structural flexibility introduced by the LRBs may cause excessive lateral movements of the viaduct superstructures during a strong earthquake. Unfortunately, these undesired lateral movements have some detrimental effects on bridge seismic performance. Hence, steel stoppers are installed to constrain the excessive lateral movements of the bridge superstructure. In this study, the bridge is equipped with stoppers graphically illustrated in **Figure 4** and **5**, where lateral side stoppers are installed on P1 and P4. The scheme of setting stoppers was originally proposed by our lab and then demonstrated as the most effective scheme with successful applications and analyses [22, 23]. As a result, the out-of-plane radial displacements are extinguished for all LRBs on P1 and P4. This scheme is also employed in the analyzed viaduct in this study. In terms of the LRBs behaviors under vertical compression, the stiffness is simply assumed as infinite in the numerical analyses. In other words, the superstructures are rigidly supported in the vertical direction. As one of essential functions of LRBs is cutting down the transferring of horizontal ground motion components from the substructures by decoupling the bridge superstructures and substructures, one may reduce the dimension of LRBs to achieve this function. As a result, the superstructures can induce a magnitude of compression stress higher than the compression strength of the LRBs. However, fortunately, this problem can be easily solved. For example, a series of auxiliary bearings which only provide vertical supports can be designed and set to ensure the feasibility of the LRBs and make the assumption of rigid vertical support available. In term of the longitudinal direction, no constraint is applied and the bridge can accommodate both the earthquake induced movements and expansions of superstructures from creep, shrinkage, and temperature fluctuations. Correspondingly, the finite element model of the curved viaduct including LRB elements and stopper elements is schematically shown in **Figure 5**.

2.2.1   LRB analytical model

To integrate the behaviors of LRBs due to transverse displacements into the analyses, a number of analytical models have been proposed [24-26], ranging from a simple equivalent linear model composed of the effective stiffness and damping ratio to a sophisticated finite element formulation reported by Salomon. In this study, a most extensively adopted trilinear force-displacement relation is employed to represent the transverse behaviors of LRBs because this model is relative simple and provides sufficient accuracy. The significant hardening behaviors of LRBs exhibited in lab tests under high shear strain levels can be captured by this trilinear model as well [27, 28]. As illustrated in **Figure 6**, the trilinear model can be characterized by five principal parameters, i.e. pre-yield stiffness K_1 which corresponds to an integral stiffness of the rubber bearing and lead plug, yielding force of the lead plug F_1, stiffness of the rubber K_2,

4

hardening force of rubber F_2, and stiffness of rubber at high strain level K_3. The hardening parameters (F_2 and K_3) are determined from fitting experimental data from shaking tests.

In this study, three LRB systems with different dimensions and properties are analyzed. **Table 1** lists all specified bearing geometries and material properties, which are provided by base isolation devices manufacturer. The three LRB systems are named as LRB-S-200, LRB-S-350, and LRB-S-500, respectively, according to their side length. To facilitate understanding the functions of based isolation LRBs and the effects of temperatures, all fixed support conditions are employed as references. Under room temperature (20°C), values of all the parameters characterizing the model are summarized in **Table 2** for these three LRBs.

2.2.2 *Temperature effect on LRB in cold regions*

At low temperatures, stiffness of the LRBs increases as a function of temperature and time, which detrimentally influence their performances. A lot of experimental investigations have been conducted to figure out the relation between the properties of LRBs and ambient temperatures. It is found that the stiffness of LRBs can even increase about 30% for the case of a long-term low temperature accumulation. Unfortunately, the area of cold regions inevitably overlaps with seismic zone, e.g. Hokkaido Island of Japan. Therefore, it is great significant to account for the low temperature effects on LRBs in seismic response analysis.

However, in an earthquake event, LRBs absorb earthquake energy and release it as heat. The heat production raises the temperature of LRBs. Thus, the stiffness variation associates with a change of temperature and time. Hence, the properties of LRBs should be defined as dynamic functions comprised of a temperature variation and a stiffness variation with respect to time and temperature, respectively.

In this study, since the real seismic/thermal coupling analysis where the data from the seismic analysis of the viaduct and the thermal analysis of the LRBs are exchanged in real time is complex, computer-intensive and time-consuming, a pseudo coupling analysis which is interpreted in details as follows is conducted. In terms of the seismic analysis, it is generally accepted that for any given instant during an earthquake the total seismic energy is balanced by the instantaneous strain energy stored in the structure, kinetic energy of moving masses, cumulative damping energy and hysteretic energy. Among these energies, the heat in LRBs is converted from the cumulative hysteretic energy. Using the FEM program coded in FORTRAN, the time histories of all these energies are obtainable from numerical seismic analysis. Hence, in the pseudo coupling analysis, Step 1, the seismic analysis is conducted without considering the dynamic properties of LRBs, which means the temperature is maintained at constant low. Step 2: the obtained numerical cumulative hysteretic energy eliminating the dynamic properties of LRBs is inputted into the lead plug of the finite element models of LRBs. Step 3: conduct thermal analysis to obtain the temperature evolution and temperature distribution of the LRBs over the period of the employed earthquake. In this study, a commercial finite element software, i.e. ANSYS, is employed for the thermal analysis. All the specified bearing properties applied in thermal analysis are supplied by the base isolation devices manufacture, as listed in **Table 1**. Taking the LRB-S-350 for instant, the FEM of 3/4 quarter of it is shown in **Figure 7(a)**, where the steel plates, rubber and lead plug are modelled with different materials and indicated by blue, purple and red, respectively. The thermal conductivity of the lead plug, rubber and steel plates are assumed as 34.9 W/(m·K), 0.3365 W/(m·K), and 55.91 W/(m·K), respectively in all analyses. These values were provided by the bearing manufacturer and are similar to the values which are normally exploited. To conduct low temperature analysis, the initial temperature of the bearing model is set as -30ºC and this low temperature is applied on all the surfaces of the bearing model from the beginning to the end of the calculation to simulate the low environment temperature. The numerical cumulative hysteretic energy time history obtained from seismic analysis is simply inputted into the FEM of the lead

plug in all the calculations considering that the energy dissipation in LRBs is primarily provided by the lead plug rather than the rubber material. Besides, it is difficult to determine or calibrate the proportions of energy absorbed by different materials of the bearing. As a result, one cannot check or evaluate the results obtained with the proportions. And then, over an earthquake duration, a convection of heat is considered between all the surfaces with the constant temperature and the lead plug which absorbs earthquake energy and release it as heat. All the temperatures mentioned in this study are absolute temperatures and not temperature differences from the construction temperature of the bridge. Correspondingly, the temperature increase and distribution in the rubber portion of the LRBs are determined based on this heat convection. As the square cross sectional LRBs is symmetrical with respect to two vertical planes passing through the central point along transverse and longitudinal directions, the temperature distributions in the four quarters divided by these two planes should identical with each other. And the temperature variation time history of the volume center can be treated as a representative of temperature states of one quarter and also the whole of the LRBs. Step 4: determine the dynamic properties of LRBs by substituting the representative temperature time history of LRBs obtained from the thermal analysis in ANSYS (Step 3) into a set of empirical LRBs properties vs. temperature relations. Based on the achievements from a cooperative research between the Rubber Bearing Association and Civil Engineering Research Institute (CERI) for Cold Region, the empirical LRBs stiffness/temperature and LRBs yield force/temperature relations are given as [29]

$$y_1 = -0.206 \times \ln(x+40) + 1.885 \tag{1}$$

$$y_2 = -0.355 \times \ln(x+40) + 2.388 \tag{2}$$

where y_1 is stiffness ratio which is equal to the instantaneous stiffness dividing the stiffness under room temperature. y_2 is yield force ratio which is equal to the instantaneous yielding force dividing the yielding force under room temperature. x is temperature. In the reference, dynamic tests of the LRBs were conducted in the Low Temperature Test Room Machine which can maintain one certain temperature with a ±0.2°C accuracy. The temperature was changed from -30° C to +40° C (-30° C→-20° C→-10° C→+23° C→+40° C), which indicated that the **Eq. (1)** and **(2)** are applicable because the tested temperature range covers the employed one in this study. Step 5: the temperature variation induced dynamic property of LRBs in cold regions is accounted for through adding a matrix substitution statement containing the dynamic properties of LRBs at the beginning of the calculation loops in the FEM analysis program coded in FORTRAN. From this seismic analysis, one can obtain the energy histories considering the temperature effects on LRBs after the first round of pseudo coupling analysis. Obviously, these energy histories should not be the same as those obtained from the real coupling analysis, but should be between the corresponding energy histories obtained from the real coupling analysis and analysis without considering the dynamic temperature effect. In order to approach the real coupling condition, more rounds of pseudo coupling analyses are required and conducted in Step 6, where the obtained cumulative hysteretic energy from the previous round is inputted into the LRBs models in the thermal analysis. Therefore, this iterative-resembled calculation stops if the difference between the energy histories obtained from the present round and the previous round is negligible compared to the absolute values of the corresponding energy histories. Finally, from this process, one can obtain the temperature distribution and representative variation time history of the LRBs. Taking the LRB-s-350 equipped viaduct subjected to a 20s duration of Kobe earthquake for instance, **Figure 7(b)** and **(c)** show the temperature distribution in the end and the temperature variation time history, respectively. In addition, the seismic behaviors of the viaducts in cold regions are obtained considering the absorbed earthquake energy induced dynamic properties of LRBs. It is found that the temperature distribution exhibits an approximately uniform radial mode. This may be understood physically as follows: (1) Over the calculations, the heat production in the lead plug is

transferred to the adjacent rubber and steel plates, which increases the temperature of the rubber and steel plates. At the same time, as the temperature of all the surface of the bearing model is set as -30°C, the thermal conduction cannot lead to a temperature increase of the rubber and steel plates in a certain distance from the surfaces. In other words, the materials in regions with a certain distance from the surfaces remain a constant -30°C of temperature. It is obvious that the effect of the low environment temperature decreases with respect to an increasing distance from the surfaces of the bearing model. Thus, in terms of the lead plug, the temperature should decrease from the center to its side, top and bottom surfaces after thermal conduction as shown in **Figure 7(b)**. (2) Even though the thermal conductivity of lead plug is much larger than that of rubber, the steel plates which sandwich together with the rubber layers have the highest thermal conductivity among the three materials. Specifically, the thermal conductivity of the steel plates is 1.6 times of the thermal conductivity of the lead plug. In addition, the thermal conduction area between rubber layers and steel plates is very large especially compared with the small thicknesses. As a result, the steel plates can absorb heat and then transfer to the adjacent rubber almost simultaneously. That is why the temperature of each rubber layer seems to be an interpolation of the temperatures of the upper and low steel plates which sandwich it as exhibited in **Figure 7(b)**. Mainly due to the above two reasons, the thermal analyses provide the approximately uniform radial mode of temperature distribution.

3 ANALYTICAL METHOD

3.1 Nonlinear dynamic equilibrium equation of motion

The analytical model of the viaduct discussed above is coded in FORTRAN. Considering that the structural damage is acceptable in current seismic design philosophies, a nonlinear dynamic analysis is conducted because the redistribution of internal actions due to the nonlinear force to deformation behaviors of all structural members can be accounted for. The governing nonlinear equation of motion can be derived following the energy principle that the external work is absorbed by the work of internal, inertial, and damping forces of all small admissible motions which satisfy compatibility and essential boundary conditions [30]. By assembling the element dynamic equilibrium equation for the time t+1 over all elements, the incremental FEM dynamic equilibrium equation can be obtained as:

$$[M]\{\ddot{d}\}_{t+1} + [C]\{\dot{d}\}_{t+1} + [K]\{\Delta d\}_{t+1} = \{F\}_{t+1} - \{F\}_t \tag{3}$$

where $[M]$, $[K]$ and $[C]$ represent the system mass, tangent stiffness and damping matrices at time t+1, respectively, whereas d, $\{\dot{d}\}$, $\{\ddot{d}\}$ denote the accelerations, velocities, and incremental displacement vectors at time t+1, respectively. $\{F\}_{t+1} - \{F\}_t$ is the unbalances force vector.

The mass matrix which is normally called as a consistent mass matrix is evaluated with the same shape functions used for the derivation of the stiffness matrix. The tangent stiffness matrix takes into consideration of the material nonlinearities and geometrical nonlinearities due to in-plane, out-plane bending, and torsional deformations. In terms of the damping matrix, as the physical causes of structural damping are very complicated, a correct representation of it cannot be formulated from a practical standpoint. In this analysis, a widely accepted simplified model, i.e. Rayleigh's damping scheme, is employed to form the damping matrix $[C]$. Accordingly, $[C]$ is formulated as a linear combination of mass and stiffness matrices. As a result, the structural damping effect can be represented by a damping coefficient which is assumed as 2% in the first two natural modes of structural vibration.

A Newmark's step-by-step integration method is used for the integration of the equation of motion from accelerations to velocities and then to the incremental displacements. For the Newmark's integration method, two parameters, i.e. γ and β, determine the accuracy and stability. The algorithm is unconditionally stable if $\beta \geq (\gamma + 0.5)^2 / 4$. In this study, 0.5 and 0.25 are assigned to γ and β, respectively,

to ensure the integration stability and optimal result accuracy. With respect to the incremental displacement $\{\Delta d\}_{t+1}$, the equation of motion is solve by a Newton Raphson iteration method, where the stiffness matrix is updated at each increment to include the geometrical and material nonlinearities.

3.2   Energy analysis

In a real seismic event, the motions of the surface of the earth, i.e. an earthquake, is actually an approach and a form of consuming and transferring the energy released in the Earth's lithosphere. As bridges are constructed on the surface, it is inevitably that certain amount of energy is transferred to and absorbed by the bridges, which is normally manifested by the earthquake induced structural damage. Although the motion of the ground at a specific site is independent of the structure built at this site, the response of the structure and the amount of energy inputted into the structure depend highly on the structural characteristics such as the natural periods of vibration and damping. According to the properties of all structural components, the inputted energy is then converted to different forms of energy including strain energy, kinetic energy, and damping energy. Therefore, the information on structural response and damage are contained in the energies. In other words, the energy provides a rational approach for evaluating earthquake induced structural responses and damages.

An energy method to quantify seismic structural responses was firstly proposed by Housner [31] where it is demonstrated that at any instant the total inputted energy equals to the summation of the kinetic energy, strain energy due to excessive structural deformations, energy dissipated by damping, and energy dissipated by permanent deformations. Zahrah and Hall [32] studied seismic energy absorption in SDOF systems, and Akiyama [33] designed steel structures based on the energy method. The energy criteria based seismic design methodology has been introduced into the Japanese Seismic Code as an effective tool in the earthquake resistance design of new structures and in the seismic assessment of the existing structures [21]. Therefore, the energy method is employed to evaluate structural damages in this study as well.

For a multi-degree-freedom system as the targeted structure in this study, the equation of motion under ground motion is given as

$$[M]\{\ddot{d}\}+[C]\{\dot{d}\}+[K]\{d\}=-[M]\{\ddot{d}_g\} \tag{4}$$

where $\{\ddot{d}_g\}$ is the earthquake induced ground acceleration vector. The energy balance equation (**Eq. (5)**) can be obtained through multiplying all terms in both sides of **Eq.(4)** by $\{\dot{d}^T\}$ and then integrating the products from the beginning of an earthquake to the concerned time (t).

$$\int_0^t\{\dot{d}^T\}[M]\{\ddot{d}\}dt+\int_0^t\{\dot{d}^T\}[C]\{\dot{d}\}dt+\int_0^t\{\dot{d}^T\}[K]\{d\}dt=\int_0^t-\{\dot{d}^T\}[M]\{\ddot{d}_g\}dt \tag{5}$$

which can be simply expresses as

$$E_K+E_D+E_S=E_I \tag{6}$$

where E_I is the total inputted energy. E_K is the kinetic energy which includes the rigid body translations of the structure. E_D represents the consumed energy due to damping mechanism of the system. E_S corresponds to the absorbed energy composed of both recoverable elastic strain energy and irrecoverable hysteretic energy. Obviously, the structure returns to the state of rest after an earthquake and **Eq. (6)** turns into

$$E_D+E_S=E_I \tag{7}$$

Hence, finally, the total energy inputted to the structure over an earthquake is dissipated by damping and inelastic deformations.

4 NUMERICAL RESULTS CONSIDERING LOW TEMPERATURE EFFECT

The analysis on the highway viaduct model is conducted using a numerical method based on the elasto-plastic finite displacement dynamic response analysis. Structural responses are examined for all selected types of bearings under the action of earthquake waves. To check the effects of low temperature and the temperature variation caused by inputted seismic energy, three temperature conditions, i.e. constant room temperature disregarding the temperature variation, low temperature including the temperature variation, and low temperature disregarding the temperature variation. For the cases using LRB-S-200, the cases under the three temperature conditions are named as s200, s200l-d, and s200l-f, respectively, and listed in **Table 3**, i.e. case 1-3. Treating the case 1 and 3 which disregard the temperature variation as references, the effects of the low temperature and the temperature variation on the seismic responses of the viaducts can be determined. Similarly, the three different temperature conditions are analyzed in cases using LRB-S-350 and LRB-S-500. In addition, a case (case 10) with fixed supporting conditions is analyzed as well to facilitate the evaluation of the base isolation effect of LRBs. As the case 10 replaces the temperature-dependent LRBs with the fixed supports, only one temperature condition, i.e. room temperature and disregarding the temperature variation, is employed. Thus, in total, 10 cases are analyzed in this section as listed in **Table 3**. Dynamic response analysis of substructure has been focused on two central piers because central piers support double weight and consequently, the most severe seismic response is normally found in this structural member.

4.1 *Employed earthquake ground motion and temperature variation of LRBs*

According to "Proposal on Earthquake Resistance for Civil Engineering Structures" issued by the Japan Society of Civil Engineers (JSCE), the earthquake is categorized into two types, i.e. Level 1 and Level 2, according to the seismic intensity. In this study, the input ground motions are accelerograms obtained during the HN Earthquake (Mw=6.9) at JR Takatori Station (TAK) during a Kobe earthquake which stuck Kobe, Japan in the 17th of January 1995 at 5:46 a.m. This earthquake is a near-fault Level 2 earthquake with a 7.2-magnitude on the Richter scale. The large magnitude of records used in this study are characterized by the presence of high peak accelerations and strong velocity pulse with a long period component as well as large ground displacements. These exceptional strong earthquakes have been selected considering their potential of causing nonlinear behaviors of the bridge. In order to evaluate the seismic performance of the viaduct, the nonlinear model is subjected to three different components of earthquake records. Acceleration histories, including the three earthquake components, are shown in **Figure 8**. The longitudinal component (*L*) of the earthquake record is selected to shake the highway viaduct parallel to the *X*-axis of the global coordinate system. This longitudinal component corresponds to the strike normal component, characterized by large pulse of motion oriented in the direction perpendicular to the fault strike, which is significantly larger than the strike- parallel or transverse component. Besides, in order to assess the effect of 3- components excitation, the transverse (*T*) and vertical (*V*) components are added simultaneously in the *Y*- and *Z*- axes, respectively. Under the employed near-fault earthquake ground motion, plastic deformation of LRBs are produced in all the employed cases. For the cases included the temperature variation, i.e. s200l-d, s350l-d and s500l-d, the employed time histories of the temperature variation are shown in **Figure 9 (a)**, **(b)** and **(c)**, respectively. As more damage or cumulative hysteretic energy can be induced in smaller dimensional of LRBs under the same ground motions, it is found that the temperature of smaller LRBs increase faster to a higher level than that of larger LRBs.

4.2 Nature vibration analysis

Over an earthquake event, the energy inputted into a structure is closely related to the correlation between the structural natural periods and earthquake dominant periods. Hence, it is of great significance to accurately calculate the natural vibration characteristics of the viaduct. In this study, owing to the introducing of base isolation system, i.e. LRBs, the structural natural periods are elongated. Characteristics of LRBs are selected following a principle that the natural periods of structures equipped with LRBs are increased to about twice the fundamental period of the same structures without LRBs. In addition, the pre-yield to post-yield stiffness ratio (K_1/K_2) is selected ensuring a moderate period shift after yielding which is recommended by Specification for Highway Bridges in Japan. And then, based on the consistent mass matrix in FEM, natural vibration analyses are conducted for the 3D viaduct model with and without LRBs. **Table 3** lists all the analytical results of viaducts equipped with the three types of LRBs under the three temperature conditions. The response spectrum of Kobe earthquake is shown in **Figure 10**. It is found that the predominant period of the earthquake locates within a range of {0.3 s, 1.4 s} which encloses the fundamental natural period of the viaduct equipped with the fixed bearings (case 10). In terms of the viaducts with LRBs under room temperatures, the fundamental natural periods are shifted away from the earthquake predominant periods. As a result, both the inputted energy into structures and the lateral forces acting substructures are expected to be decreased.

From **Table 3**, one can clearly observe the influence of bearing support on natural vibration characteristics, which is mainly due to the horizontal stiffness of the bearings. For all the selected cases, the fundamental natural period corresponds to the mode shape along the viaduct longitudinal direction. Compared to the case 10, the cases have closer periods indicate that the support conditions of these case cannot provide the strong capability of shifting the structural fundamental natural period away from the dominant period ranges of the inputted ground motions as those of other cases. Thus, the listed results demonstrate that the natural period shifting capability of LRBs is weakened due to the low temperature. However, even though the natural period increases with a decreasing horizontal stiffness of bearings, a large horizontal motion of superstructures may occur during an earthquake if bearings with too small stiffness are installed. Thus, a moderate period shift (with a maximum period ratio to all fixed supporting condition equaling to about 2.0) are accounted for to ensure that the displacements of superstructures satisfy the requirements of codes during strong earthquakes.

4.3 Shear force-displacement response at bearing

In highway viaducts, the bearings connect the superstructures and substructures through transferring forces, especially shear force, and displacements during an earthquake. On one hand, the peak shear force transmitted from superstructures to piers tops should be controlled to keep the bending moment at the base of piers in an acceptable range. On the other hand, it is essential to obtain moderate maximum shear displacements at bearings to avoid large peak superstructure displacements which may result in pounding between substructures and abutments. Even if no pounding occurs, oversize displacements may result in an insufficient clearance between bridge decks and abutment at the expansion joints, which is detrimental to the serviceability of the bridges. Thus, the capability of transferring shear forces and displacements determines the overall seismic behaviors of the highway viaducts. And, the shear force-displacement relationships at bearings are an important indicator for structural seismic performances.

As the center piers are more vulnerable than the side piers, the shear force-displacement responses of bearing support P3 are shown in **Figure 11**. It can be found that the shear force-displacement response is not smooth and presents 1 to 3 number of steps for different cases. These steps correspond to the steps of the employed trilinear force-displacement analytical model of LRBs (see **Figure 6**). Taking the cases

equipped with LRB-S-200 for example, for the case under room temperature (s200), it is found that the forces of the demarcation points for step 1 to step 2 and step 2 to step 3 are about 63kN and 125kN, respectively, which are the same as the F_1 and F_2 listed in the **Table 2** for the LRB-S-200. Nevertheless, due to the low temperature effect, the yield forces are increased according to **Eq. (2)**. Consequently, the three steps are not observed in the responses of the cases s200l-d and s200l-f. Similarly, the steps of other responses can be understood. Focusing on the cases in any column where the viaducts are equipped with the same type of LRBs, it is found that the maximum inertial force transmitted to LRBs increases with increasing temperature whereas the maximum displacement of LRBs exhibit an opposite trend with respect to the temperature. Specifically, it can be observed that piers under low temperature sustains about 5-13% of inertial force more than piers under room temperature. Meanwhile, the deformation of LRBs under low temperature experiences about 11-20% of displacement less than the same device under room temperature. These negative phenomena are attributed to the stiffness variation caused by the temperature dependence of rubber material. Moreover, it should be emphasized that one of the essential seismic protecting mechanism of LRBs is deforming to dissipate the earthquake energy, which is represented by the area enclosed by the hysteresis loops. Compared with the loops of constant low temperature cases, the area of loops is increased to about 2 times if the temperature variation is accounted for, especially for the cases using LRB-S-200 where the base isolation effect of bearings is more fully implemented. Thus, the detrimental effects of low temperature can be alleviated by the absorbed earthquake energy induced-LRBs temperature variation. And, this alleviating effect becomes more obvious if the earthquake is intensive enough to induce significant plastic deformations in LRBs. In other words, the more severe the earthquake-induced damage to LRBs is the more alleviating effects can be provided by the LRBs. Besides, if the three response curves in the same raw are investigated jointly, one can find that the maximum inertial force transmitted by the LRBs increases, whereas and the maximum displacement of LRBs decreases with the increasing LRBs dimension or stiffness, respectively. In addition, comparing results of LRB cases with those of fix supported cases, it is clear that the LRBs can evidently reduce inertial forces acting on bridge pies which are also an important function of the base isolation system. However, some unfavorable effect of low temperature on the efficiency of LRBs, such as the increment of bearing stiffness and peak shear force acting on piers and the reduction of bearing deformation, can be clearly observed as well.

4.4 Bending moment-curvature response

In most cases, structural damage due to earthquakes can be attributed to the plastic hinges formed at the bases of bridge piers [20]. As the bottoms of bridge piers are subjected to the maximum moments due to earthquakes, the failure usually starts from a local plate buckling in those regions represented by the form of plastic hinges. Therefore, the bending moment at the base of bridge piers is a good measure for quantifying the damage level of bridges induced by the earthquake. Moment-curvature loops at base of pier (P3) are plotted in **Figure 12** for viaducts supported on the different types of bearings listed in **Table 3**. With the geometrical dimensions and material properties of piers, the yielding moment of bridge piers is determined as 84.8 MN·m. Thus, inelastic deformations occur in all cases.

In **Figure 12** in the first raw where all LRB bearings with different geometrical sizes are under room temperature, it is found that the maximum bending moment overpasses the yield moment of piers for about 4% - 5%, and correspondingly piers behave almost linearly, whereas in the second and third raw, apparent inelastic deformations are observed in piers under low temperature regardless of including or excluding the temperature variation. Due to the inelastic deformations, the loops cannot return to their origin positions. The shift from the origin position and the position after restoring demonstrates the existence of plastic hinges at the pier base. Comparing the loops of cases under low temperature include/exclude the temperature variation, it can be found that the plastic deformation is apparently reduced if the absorbed

earthquake energy induced-temperature variation is accounted for, which emphasizes the significances of this research. Moreover, if figures in a same raw are analyzed jointly, a consistent orderliness can be found for LRB bearings with different dimensions, which is that the degree of inelastic deformation increases with the increasing dimension of the LRB bearings. This is because the larger size of bearings is stiffer resulting in more forces transferred between the super- and sub-structures. In addition, it should be mentioned that the damage to piers can be controlled in a relatively low level even under low temperature condition if the base isolation system is designed appropriately. This conclusion can be deduced from figures in the first row.

4.5 Energy time history

In the last few decades, an energy concept have been advised as an effective alternative approach to the traditional design strategies for the identification of seismic damages imposed by earthquakes to structural members in [34, 35]. Generally, this concept can be simply expressed by an energy balance equation presented in Section 3.2, where the seismic input energy is assumed as equaling to a summation of kinetic, plastic strain, and damping energies. However, the kinetic energy consisting of the rigid body movements of all structural members can be regarded as negligible at the end of an earthquake. Therefore, recently Bertero et al. [36] presented a conceptual methodology for earthquake resistant design, where the total input energy and energy dissipated as damping energy and plastic hysteretic energy are considered simultaneously. For the cases in this study, this plastic hysteretic energy which represents the structural damages [37] includes the absorbed energy by the hysteresis loops of steel bridge piers and the hysteretic energy dissipated by the bearings.

The obtained results (see **Figure 13**) show that the amount of seismic energy inputted into the viaduct depends highly on the structural characteristics such as the fundamental period of vibration and damping properties. In comparing the energy-time histories for the two temperature conditions, it is remarked that the seismic energy dissipated by the same base isolation system under room temperature is always larger than that of low temperature.

Focusing on figures in the first column where LRB bearings with the same dimension are subjected different temperature conditions, it is found that the total strain energy from plastic deformations in both piers and bearings decreases with a reduction of temperature. However, the strain energy absorbed by the plastic deformation of piers exhibited an opposite trend with respect to the variation of temperature as shown in **Figure 13**. These phenomena mean that LRB systems under room temperature can dissipate more strain energy before causing plastic deformation or damage in bridge members than those under low temperature, which deomonstrates the base isolation function of LRB bearings is more fully realized under room temperature. This is the essential of a seismic isolation method which is controlling the seismic response of structures through yielding of the isolators. The effect of this yielding on the seismic response is to reduce the load for which a structure must be designed to resist seismic forces. And this decrement of strain energy dissipation is definitely an unfavorable phenomenon caused by the low temperature.

4.6 Displacement time history at top of piers

Bridge structures should not only remain standing but also be usable after a large earthquake otherwise society may suffer a huge economic loss and serious inconvenience. Based on the experiences in 1995 Hyogoken-Nanbu earthquake, a large number of bridge piers survived without collapse exhibited large residual displacements at their tops which made the structures unusable, unsafe, and in some cases irreparable. A check of residual displacement of bridge piers after the Hyogoken-Nanbu earthquake concluded that about 100 piers with a tile angle more than 1/100 (rad) of degree had to be demolished [38].

In this study, the residual displacement at pier top is exploited as an indicator of structural damage during an earthquake. For all cases, displacement-time histories at the top of piers (P3) are shown in **Figure 14** to evaluate the final position of piers relative to the original. According to the Specifications for Highway Bridges in Japan [21], the allowed residual displacement is 1/100 of the height from the bottom of bridge piers to the point on the superstructure where the inertial force acts on, or in other words, the rotation angle of bridge piers should be small than 1/100 (rad). Restoration work may be difficult to conduct as a large residual displacement is generated in the substructure after an earthquake.

Under room temperature, moderate peak responses are observed for any analytical models with different bearing conditions. For the residual displacement, small values are obtained for systems equipped with LRBs: 0.1 cm for LRB-S-200 (case 1), 0.2 cm for LRB-S-350 (case 4) and 0.2 cm for LRB-S-500 (case 7). Scarcely residual displacements observed in these cases indicate that almost all structural elements function well under room temperature. But in the cases of low temperature considering temperature variation, displacement responses at the top of piers are sensibly increased. In terms of the residual displacement, even for piers equipped with LRBs, considerable residual displacements are observed as: 1.2 cm for LRB-200 (case 2), 2.4 cm for LRB-S-350 (case 5) and 3.9 cm for LRB-S-500 (case 8), due to the curvature originated at pier bases. It is found that the residual displacement shows a positive correlation with the bearing dimension, which further emphasizes that the large size of LRBs cannot ensure good performance and the LRB systems should be designed on a case-to-case basis. However, there should be a suitable LRBs system which can provide sufficient energy dissipation function, and control the transferred force between super- and sub-structures and further residual displacement at pier tops in an acceptable range for a given bridge subjected to a target or design earthquake magnitude. The residual displacement can be even more remarkable if the temperature variation is not included in the analyses. Moreover, residual displacement which is caused by the residual curvature generated by inelastic deformation at the pier base and deformation of base isolator could only be observed in the worst case (case 7) among the cases under room temperature. This result means that a proper designed base isolation system works well under room temperature, whereas under low temperature, residual displacement is observed in all the cases. And the maximum displacement increases simultaneously. This is one more unfavorable effect of low temperature. Correspondingly, considerations of the low temperature effects should be concerned in the design of LRB systems.

5 NUMERICAL RESULTS UNDER LONG DURATION EARTHQUAKE

Even though the intensity of the employed earthquake ground motions in 1995 Kobe earthquake is strong enough to cause hysteretic energy in LRBs, the lasting time (20 seconds) is too short to ensure enough heat production in bearing supports. As a result, the temperature of LRBs rose up to only -10℃ and only a slight variation of bearing properties was observed. In order to extend the application range of low temperature effect investigation, earthquakes with long duration of 1 minute are employed in this section. As the focus is the effect of earthquake duration, the LRB-S-350 is used in all cases. Under such long duration earthquakes, the temperature of LRBs is expected to be raised more remarkably. And then, more comprehensive conclusions of low temperature effects on seismic responses can be obtained through jointly investigating the results of both sections.

5.1 *Employed earthquake ground motions and temperature variation of LRBs*

A strong ground motion recorded at the Hiroo Machi (HKD 100) during the 2003 Tokachi-Oki earthquake are considered as proper records and adopted in this study because the tremors lasted for approximately 2 minutes. **Figure 15** shows the first one minute of the earthquake ground motion records along longitudinal (*L*), transverse (*T*), and vertical (*V*) directions. Actually, the Hiroo Machi is an earthquake-prone region

in the cold Hokkaido Island. As the Epicenter of the earthquake, offshore of Tokachi, was more than 80 km away from the Hiroo Machi, the seismic magnitude of the recorded ground motions is only M6.0 which is much smaller than the magnitude at the Epicenter of the earthquake (M8.2). Under this M6.0 of ground motions, almost no damage can be produced in the structural members and LRBs of the viaduct. In other word, the heat generation and the induced temperature variation in LRBs can be regarded as negligible. However, it is expected that an earthquake with similar or even higher magnitude may occur under the mainland in future. Therefore, earthquake ground motions with a triple magnitude of the corresponding ground motions in **Figure 15** are employed as well. These amplified ground motions are expected to cause more damage to the LRBs to facilitate the evaluation of seismic performance of LRBs under low temperatures. Therefore, this section employs three sets of earthquake ground motions, i.e. 1995 Kobe earthquake, 2003 Tokachi-Oki earthquake, and triple of the 2003 Tokachi-Oki earthquake. Under each set of earthquake ground motions, the same three temperature conditions as in section 4 are analyzed. Consequently, 10 cases are analyzed in this section including the fixed support case as listed in **Table 4**. Moreover, the temperature variation time histories of the LRB-s-350 are show in **Figure 16 (a)** and **(b)** for the viaduct subjected to the ground motions recorded in 1995 Kobe earthquake and triple of the ground motions recorded in 2003 Tokachi-Oki earthquake, respectively. It can be found that due to the absorbed earthquake energy the LRBs temperature can be more remarkably increased if the viaduct is subjected to the 1-minute long duration of earthquake ground motions than that subjected to the 20s short duration of earthquake ground motions.

5.2   Natural vibration analysis

The results obtained from natural vibration analyses are summarized in **Table 4** for all the employed conditions. It should be mentioned that, for dynamic stiffness cases including the temperature variation, nature frequency also varies during earthquake, and only one intermediate value is listed here considering the limited space. Since stiffness of LRBs increases under low temperature, low temperature cases (2, 3, 5, 6, 8, 9) have shorter natural periods than room temperature cases (1, 4, 7). This means low temperature weakens the base isolation function by hardening the rubber material. Compared with the constant low temperature conditions, the dynamic stiffness cases (temperature increases during earthquake) perform better. In addition, it is found from the response spectrum of earthquake wave (**Figure 17**) that the predominant periods locate from 0.1s to 1.0s. Thus, the base isolation system successfully shifts the bridge fundamental natural periods away from the predominant earthquake periods.

5.3   Shear force-displacement response at bearing

Figure 18 shows the shear force-displacement relationship at bearing. It is found that, under low temperature condition especially fixed -30℃ condition, LRBs deformation decreases. Correspondingly, the area of the hysteresis loops which represents the additional energy absorbing ability provided by bearing systems decreases as well. This reduction of area of the hysteresis loops results in a deterioration of base isolation function. In addition, focusing on any column of curves in **Figure 18**, the maximum response force exhibits an increasing trend from top to bottom, which means the isolation effect of LRBs is weakened. This is caused by the decreased flexibility and shortened natural period under low temperature. Benefiting from the properly selected base isolation system, the hardening effect which should be avoided as suggested by specifications is not observed in all the cases.

To investigate the effect of earthquake duration, attentions should be focused on the second and third columns as slight damage (area of hysteresis loop) is observed in all cases (case 1, 2, 3) under the original Tokachi-Oki earthquake. The effect of low temperature cannot be manifested under this original Tokachi-Oki earthquake as well. As for the hysteresis loops in the second and third columns, even though they

show similar trends with respect to the variation of temperature conditions, it is found that the area difference between room temperature cases and low temperature case is more apparent under the short duration Kobe earthquake (case 7, 8, 9) than under the long duration triple amplified Tokachi-Oki earthquake (case 4, 5, 6). This is owing to the more heat production and related temperature increasing under longer durations of earthquake. Therefore, it is clearly indicated that the earthquake induced heat production can alleviate the detrimental effect of low temperature on the performances of base isolation systems to certain extend if its duration is long enough.

5.4   Bending moment-curvature response at pier base

As the bending moment-curvature response at the base of piers is a good indicator for evaluating the level of earthquake induced damage, the bending moment-curvature response for all cases are shown in **Figure 19**. It is clearly shown that a proper selection of LRBs can effectively reduce inertial forces acting on bridge piers, which is one of the most important objectives of setting base isolation systems. In this study, the yielding moment of the pier is calculated as 84.8 MN·m. Thus, inelastic deformation which represents the damage on piers occurs in all low temperature cases under the triple amplified Tokachi-Oki earthquake and the Kobe earthquake. Even though an inelastic behavior is acceptable in present specifications for severe or near-fault earthquakes, this inelastic deformation is actually caused by the detrimental effect of low temperature on the performance of LRBs rather than the magnitude of earthquake. This means the LRBs designed following the present specifications without considering the low temperature effects may lead to some unexpected structural damage under low temperatures, which demonstrates the necessities of considering the low temperature effects in cold regions seismic design regardless of long or short duration earthquakes.

5.5   Energy-time history

The time histories of all kinds of energies including the total inputted energy, kinetic energy, damping energy, and strain energy are shown in **Figure 20** for all analyzed cases. For bridge equipped with LRBs, the total earthquake energy is increased due to the large seismic energy dissipation at the LRBs. As the total strain energy is from the inelastic deformation of LRBs and structural members, whereas the strain energy dissipated by the piers deceases under low temperature conditions as shown in **Figure20**. Hence, the increased total strain energy is dissipated by the LRBs instead of by the structural members. In other words, the LRBs sacrifice themselves to protect the other structural members. As a result, the seismic damage is considerably reduced. Due to the stiffness increasing and the weakened isolation function of LRBs under low temperature, the strain energy which represents the energy dissipation mechanism by hysteresis loops at bearings decreases significantly. Thus, the inelastic behavior at piers absorbs earthquake energy, which results in more structural damage in these cases. This is coincident with the other results from analysis.

Focusing on the energy time histories of the triple amplified Tokachi-Oki earthquake and the Kobe earthquake, it is found that the amount of energy dissipation decreases under low temperature for both earthquakes. Thus, the deteriorated energy dissipation capability of LRBs may cause unexpected serious damage if a bridge confronts certain extreme strong earthquakes. Specially, the low temperature caused strain energy decreasing is more remarkable for the Kobe earthquake than the triple amplified Tokachi-Oki earthquake, which means the LRBs experience more functionality lost under a shorter duration earthquake.

5.6   Displacement time history at top of piers

Finally, the displacement time histories at the tops of piers are shown in **Figure 21**, where the residual displacement can be also observed. This permanent residual displacement affects the post-earthquake serviceability of highway viaducts severely. Accordingly, specifications prescribed residual displacement limitation which is 1/100 of pier height. From **Figure 21**, the effect of earthquake duration can be clearly observed because an over-limitation residual displacement (larger than 0.2 m) occurs only for the Kobe earthquake and under low temperature conditions. As for the long duration earthquake, no apparent variation of residual displacement is observed from case 4 to case 6.

6 CONCLUSIONS

In this study, exploiting a FEM based nonlinear dynamic numerical method, the effects of the low temperature and the absorbed earthquake energy induced temperature variations on the base isolation performances of Lead Rubber Bearings (LRBs) are evaluated and figured out by investigating the seismic responses of a curved highway viaduct equipped with LRBs under three different temperature conditions, i.e. room temperature, low temperature including/excluding the temperature variations. In this method, both geometrical and material nonlinearities were included for structural members including bridge piers and LRBs. In addition, a dynamic bearing property definition was introduced to practically simulate the temperature variation and property variation of LRBs with respect to time and temperature, respectively, during an earthquake event.

Under the three different temperature conditions, the seismic responses of the bridge viaduct equipped with three dimensions of LRBs are calculated employing a set of near-fault Kobe earthquake motions with a 20s duration. The results demonstrated that the LRBs, especially the smaller LRBs, can significantly reduce the seismic forces acting on structural members, whereas the base isolation function was dramatically weakened due to a stiffness increase of LRBs under low temperature conditions. Moreover, the detrimental low temperature effect was alleviated by the temperature variation. And, the alleviating effect was more apparent for smaller LRBs because the earthquake can create more plastic deformation and generate more energy in them. Consequently, the earthquake induced structural damages which were exhibited as residual displacement and known as plastic hinge at the bases of bridge piers increased with the increasing size of LRBs and the decreasing temperature. Therefore, on the basis of satisfying the limitations of superstructure displacement, the LRBs in viaducts, especially for the ones located in the Cold Regions, are suggested to be employed jointly with auxiliary bearings, where the LRBs should be designed with relatively small dimensions or lateral stiffness to ensure sufficient heat generation during the target earthquake magnitude and the auxiliary bearing can be designed to provide enough vertical supports.

Considering that the temperature variation is dependent on the earthquake duration, two long duration (60s) of earthquakes, i.e. original and triple amplified Tokachi-Oki earthquake, were employed jointly with the short duration earthquake as well to deepen the understanding of the effect of temperature variation. Under the triple amplified Tokachi-Oki earthquake, the absorbed energy by the LRBs for the low temperature case including temperature variation was increased to about half of that for the room temperature case and two time of that for the low temperature case disregarding temperature variation. Compared with the structural responses under the short duration of earthquake, the remarkably increased energy absorption under the long duration of earthquake resulted in more apparently reduced shear force transmitted by the LRBs, bending moment at pier base and residual displacement at pier top. These phenomena demonstrated the necessities of including the dynamic bearing property over an earthquake to achieve an accurate seismic analysis of bridge viaducts located in cold regions.

In summary, the low temperature effect and the temperature variation in LRBs should be accounted for in designing the LRBs of bridge viaducts located in cold regions, accordingly the LRBs may be designed with smaller size or lateral stiffness than those for non-cold regions. Additionally, in order to realize an accurate seismic analysis of the bridge viaducts, the property variation of LRBs over an earthquake should be comprehensively considered.

REFERENCES

[1] Abdel-Salam, M. N., & Heins, C. P. (1988). Seismic response of curved steel box girder bridges. Journal of Structural Engineering, 114(12), 2790-2800.

[2] Desroches, R., & Fenves, G. L. (1997). Evaluation of recorded earthquake response of a curved highway bridge. Earthquake Spectra, 13(3), 363-386.

[3] Hayashikawa, T., Otake, A., and Nakajima, A. (1998). Nonlinear behavior of curved viaducts subjected to three-dimensional earthquake ground motions. Paper No. G1-20, The 10th Earthquake Engineering Symposium Proceedings, Architectural Institute of Japan, Tokyo, Japan, 2, 202-216.

[4] Hashimoto, S., Fujino, Y., & Abe, M. (2005). Damage analysis of Hanshin Expressway viaducts during 1995 Kobe earthquake. II: Damage mode of single reinforced concrete piers. Journal of Bridge Engineering, 10(1), 54-60.

[5] Rose, A., & Lim, D. (2002). Business interruption losses from natural hazards: conceptual and methodological issues in the case of the Northridge earthquake. Global Environmental Change Part B: Environmental Hazards, 4(1), 1-14.

[6] Kunde, M. C., & Jangid, R. S. (2003). Seismic behavior of isolated bridges: A-state-of-the-art review. Electronic Journal of Structural Engineering, 3(2), 140-169.

[7] Buckle, I. G., & Mayes, R. L. (1990). Seismic isolation: history, application, and performance—a world view. Earthquake spectra, 6(2), 161-201.

[8] Kelly, J. M. (1986). Aseismic base isolation: review and bibliography. Soil Dynamics and Earthquake Engineering, 5(4), 202-216.

[9] Bessason, B., & Haflidason, E. (2004). Recorded and numerical strong motion response of a base-isolated bridge. Earthquake Spectra, 20(2), 309-332.

[10] Ozdemir, G., Avsar, O., & Bayhan, B. (2011). Change in response of bridges isolated with LRBs due to lead core heating. Soil Dynamics and Earthquake Engineering, 31(7), 921-929.

[11] Ozdemir, G., & Dicleli, M. (2012). Effect of lead core heating on the seismic performance of bridges isolated with LRB in near‐fault zones. Earthquake Engineering & Structural Dynamics, 41(14), 1989-2007.

[12] Chaudhary, M. T. A., Abe, M., Fujino, Y., & Yoshida, J. (2000). System identification of two base-isolated bridges using seismic records. Journal of Structural Engineering, 126(10), 1187-1195.

[13] Park, K. S., Jung, H. J., & Lee, I. W. (2002). A comparative study on aseismic performances of base isolation systems for multi-span continuous bridge. Engineering Structures, 24(8), 1001-1013.

[14] Jangid, R. S., & Kelly, J. M. (2001). Base isolation for near‐fault motions. Earthquake Engineering & Structural Dynamics, 30(5), 691-707.

[15] Oshima, T., Mikami, S., Yamzaki, T., Ikenaga, M., Matsui, Y., & Kubo, K. (1998). Experimental of functional confirmation on lead rubber bearing (LRB) under low temperature. Journal of Structural Engineering, 44A, 753-760.

[16] Khan, A. S., & Lopez-Pamies, O. (2002). Time and temperature dependent response and relaxation of a soft polymer. International Journal of Plasticity, 18(10), 1359-1372.

[17] Hayashika, T. (2000) Bridge Engineering. Asakura Publication Co., Ltd.

[18] Bates, R. E., & Bilello, M. A. (1966). Defining the cold regions of the northern hemisphere (No. TR-178). Cold Regions Research and Engineering Lab Hanover NH.

[19] Liu, Q., Kasai, A., & Usami, T. (2001). Two hysteretic models for thin-walled pipe-section steel bridge piers. Engineering Structures, 23(2), 186-197.

[20] Hsu, H. L., & Chang, D. L. (2001). Upgrading the performance of steel box piers subjected to earthquakes. Journal of Constructional Steel Research, 57(9), 945-958.

[21] Japan Road Association. (2002). Specification for Highway Bridges, Part V: Seismic Design. Tokyo, Japan.

[22] Tanaka, R., Galindo, C. M., & Hayashikawa, T. (2009). Nonlinear seismic dynamic response of continuous curved highway viaducts with different bearing supports. World Academy of Science, Engineering and Technology, 5, 327-333.

[23] Tian, Q., Hayashikawa, T., & Ren, W. X. (2016). Effectiveness of shock absorber device for damage mitigation of curved viaduct with steel bearing supports. Engineering Structures, 109, 61-74.

[24] Hwang, J. S., & Chiou, J. M. (1996). An equivalent linear model of lead-rubber seismic isolation bearings. Engineering Structures, 18(7), 528-536.

[25] Salomón, O., Oller, S., & Barbat, A. (1999). Finite element analysis of base isolated buildings subjected to earthquake loads. International Journal for Numerical Methods in Engineering, 46(10), 1741-1761.

[26] Kikuchi, M., & Aiken, I. D. (1997). An analytical hysteresis model for elastomeric seismic isolation bearings. Earthquake Engineering & Structural Dynamics, 26(2), 215-231.

[27] Ruiz Julian, F. D., and Hayashikawa, T. (2004). Effect of hardening of lead-rubber bearings on nonlinear behaviour of highway viaducts under great earthquakes, Proceedings of 13th World Conference on Earthquake Engineering, CD-ROM, Paper No. 3332, Vancouver, Canada.

[28] Sato, N., Kato, A., Fukushima, Y., & Iizuka, M. (2002). Shaking table tests on failure characteristics of base isolation system for a DFBR plant. Nuclear Engineering and Design, 212(1-3), 293-305.

[29] Imai, T., Satoh, T., Nishimura, T., Tanaka, H., and Mitamura, H. (2008). The performance evaluations of rubber bearings for bridges in cold districts. Proceeding of Hokkaido Chapter of JSCE, Vol.64, A-18.

[30] Ali, H. M., & Abdel-Ghaffar, A. M. (1995). Modeling the nonlinear seismic behavior of cable-stayed bridges with passive control bearings. Computers & Structures, 54(3), 461-492.

[31] Housner, G. W. (1959). Behavior of structures during earthquakes. Journal of the Engineering Mechanics Division, 85(4), 109-130.

[32] Zahrah, T. F., & Hall, W. J. (1984). Earthquake energy absorption in SDOF structures. Journal of Structural Engineering, 110(8), 1757-1772.

[33] Akiyama, H. (1985). Earthquake-resistant limit-state design for buildings. Univ of Tokyo Pr.

[34] Decanini, L. D., & Mollaioli, F. (2001). An energy-based methodology for the assessment of seismic demand. Soil Dynamics and Earthquake Engineering, 21(2), 113-137.

[35] Bruneau, M., & Wang, N. (1996). Some aspects of energy methods for the inelastic seismic response. Engineering Structures, 18(1), 1-12.

[36] Bertero, R. D., & Bertero, V. V. (2002). Performance‐based seismic engineering: the need for a reliable conceptual comprehensive approach. Earthquake Engineering & Structural Dynamics, 31(3), 627-652.

[37] López, O. A. (2000). Plastic energy dissipated during an earthquake as a function of structural properties and ground motion characteristics. Engineering Structures, 22(7), 784-792.

[38] MacRae, G. A., & Kawashima, K. (1997). Post‐earthquake residual displacements of bilinear oscillators. Earthquake Engineering & Structural Dynamics, 26(7), 701-716.
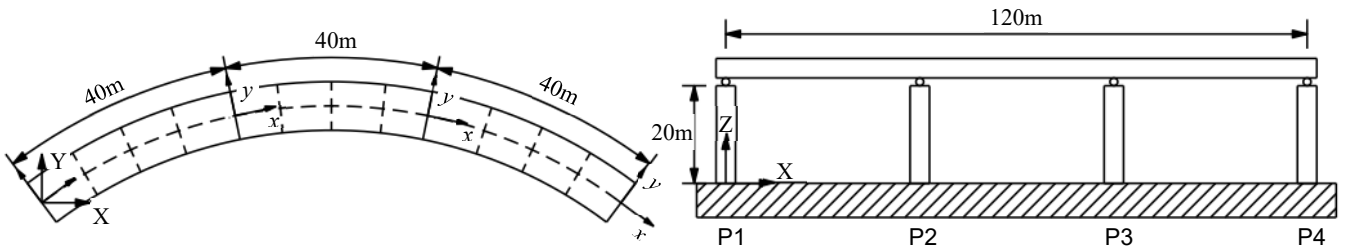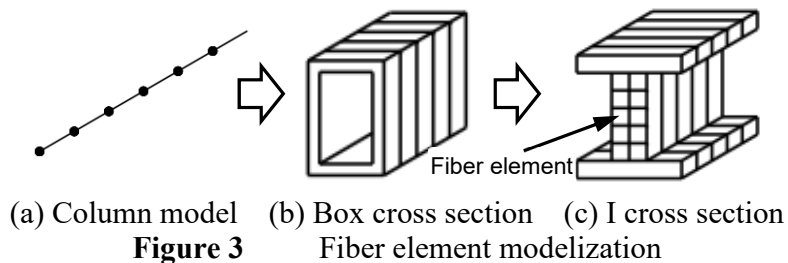
FIGURES

(a) Plane view of the curved highway viaduct   (b) Elevation view of the curved highway viaduct

Figure 1   Analytical model of the viaduct
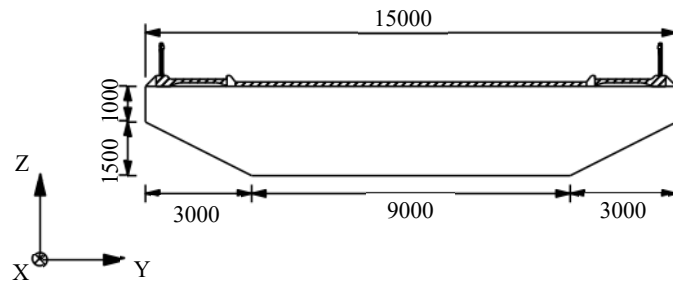
Figure 2   Cross section of superstructure (Unit: mm)

(a) Column model   (b) Box cross section   (c) I cross section
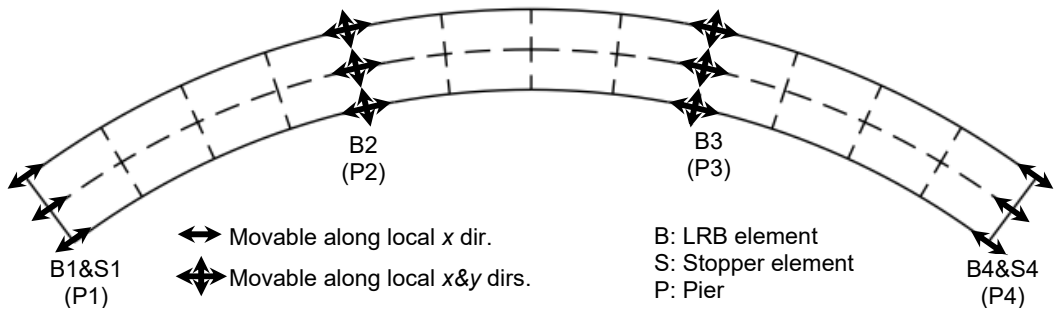
Figure 3   Fiber element modelization
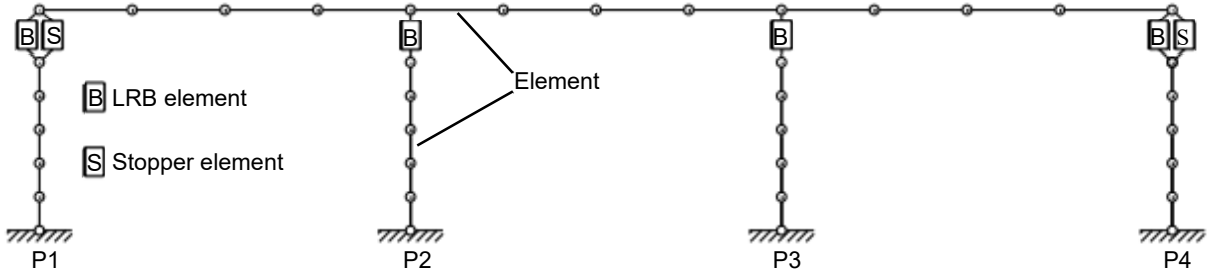
Figure 4   Restraint configurations of LRBs

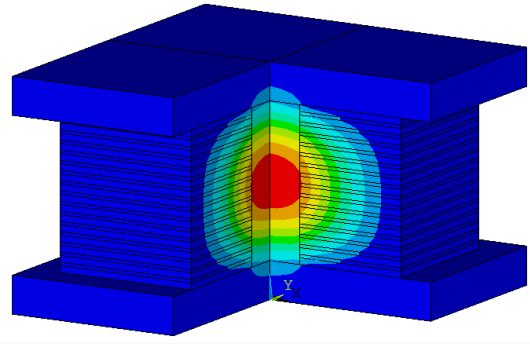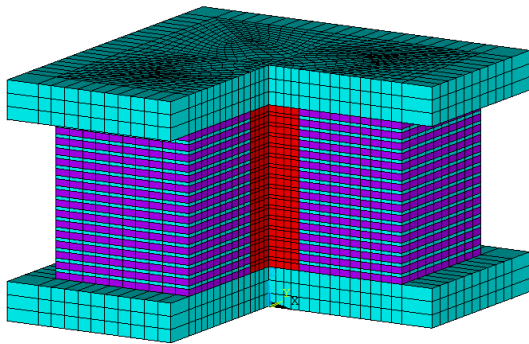**Figure 5**   Elevation view of the viaduct finite element model
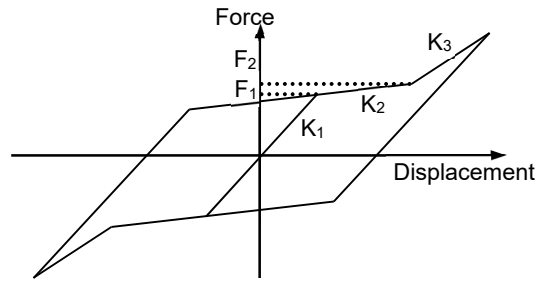
Figure 6   Analytical model of LRBs

20
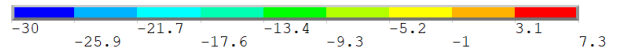
(a) FEM   (b) Temperature distribution
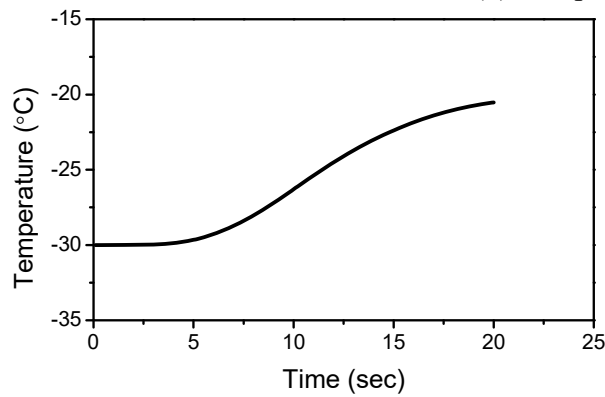
(c) Temperature variation time history

Figure 7   Thermal analysis of LRB-S-350 under 20s of Kobe earthquake
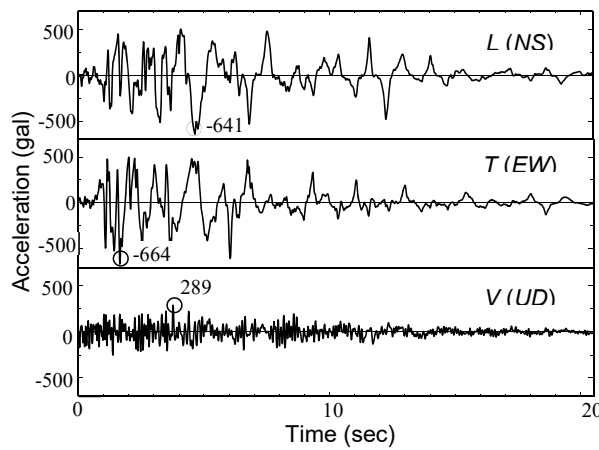
Figure 8   Kobe earthquake accelerations

21
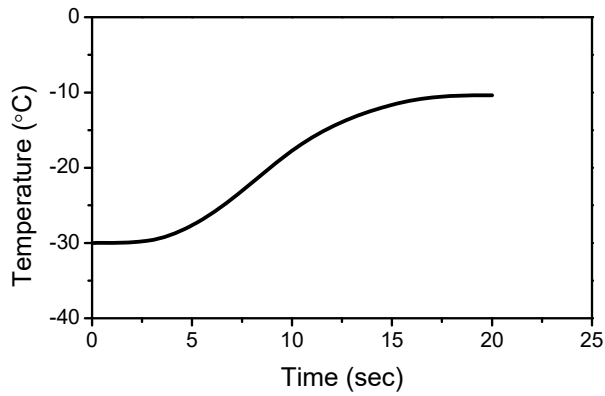
(a) case s200l-d
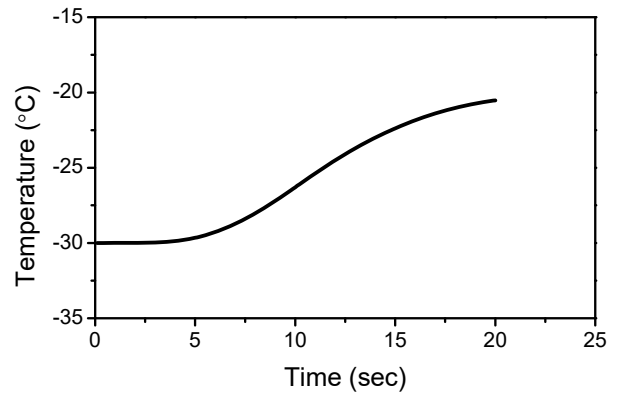
(b) case s350l-d
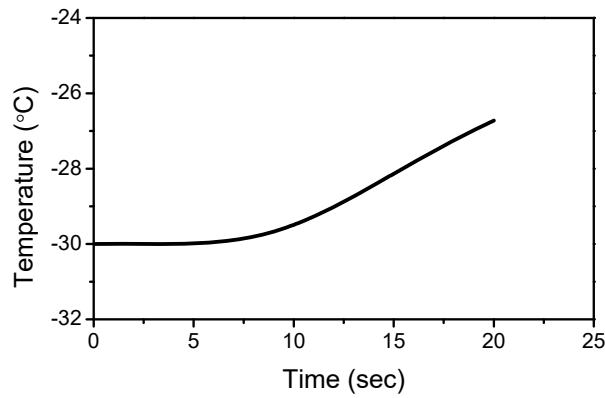
(c) case s500l-d

Figure 9　　　　Time histories from thermal analysis
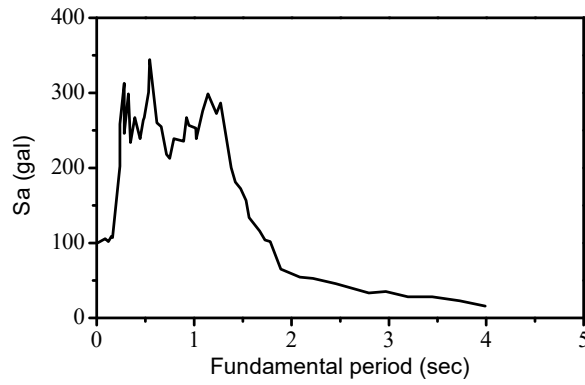
Figure 10　　　　Response spectrum of Kobe earthquake, *L* (*NS*)

22
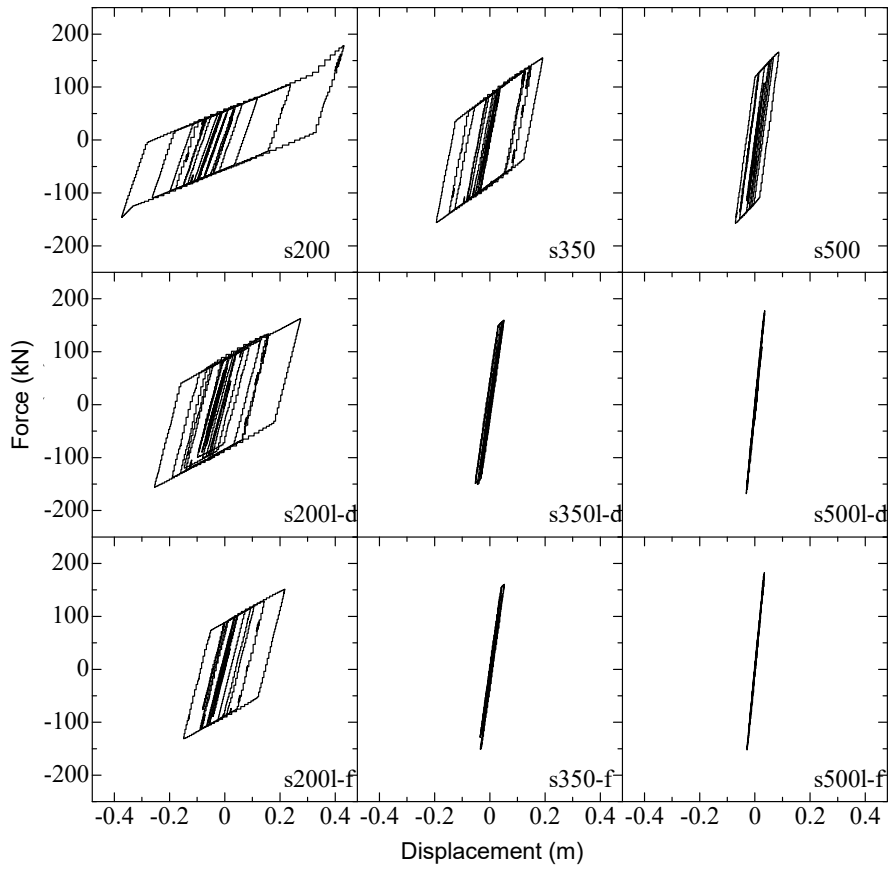
Figure 11   Shear force-displacement response at bearing (P3 *X*-direction)
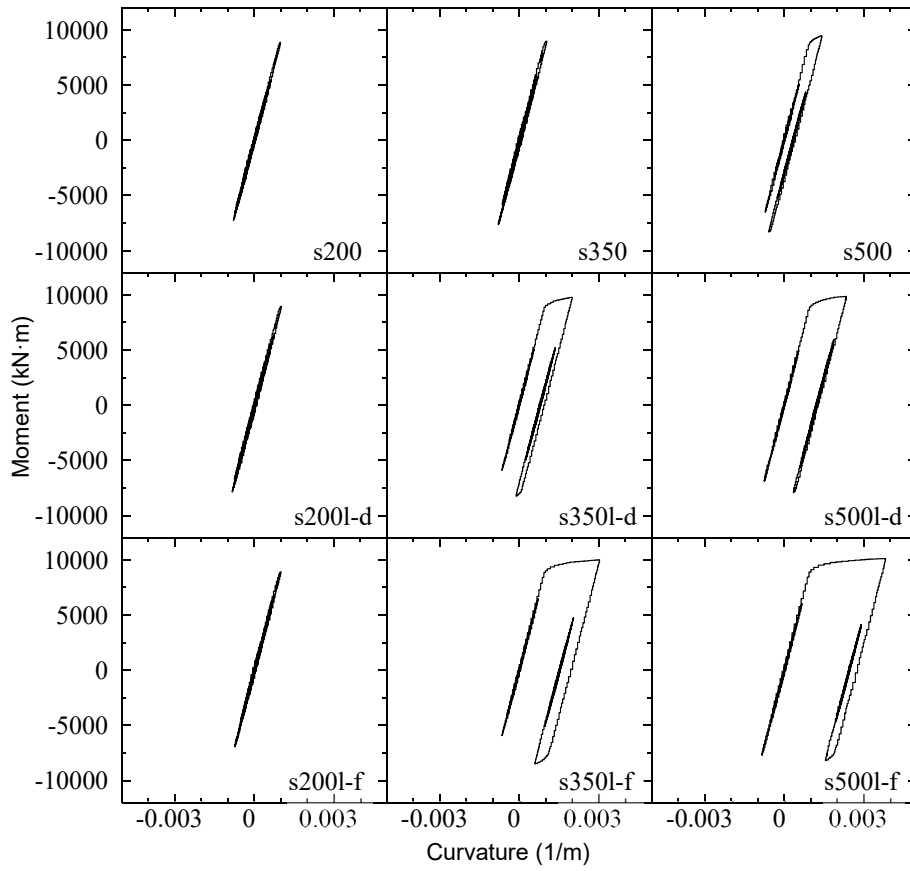
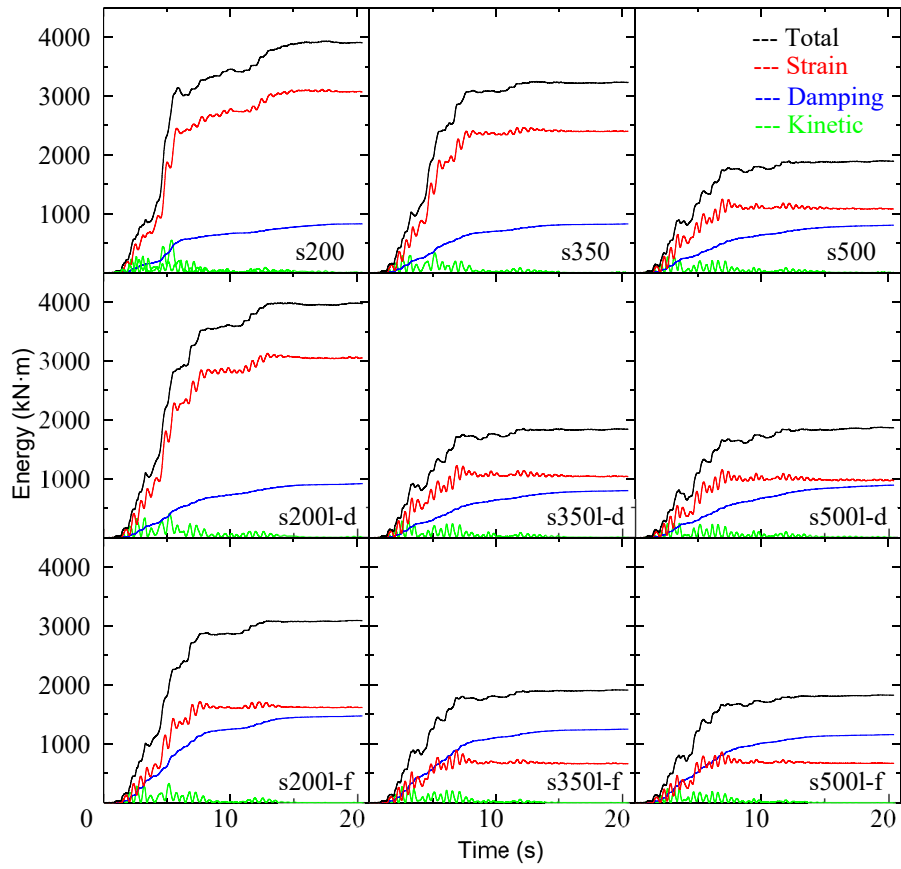**Figure 12**   Bending moment-curvature response (P3 *X*-direction)

Figure 13   Energy time history

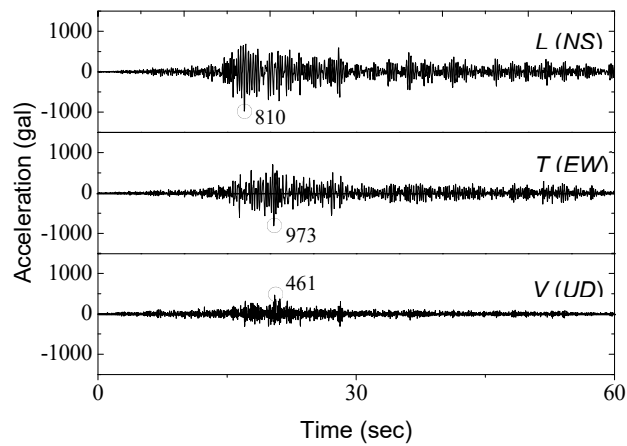**Figure 14**   Displacement-time history at top of piers (P3 *X*-direction)

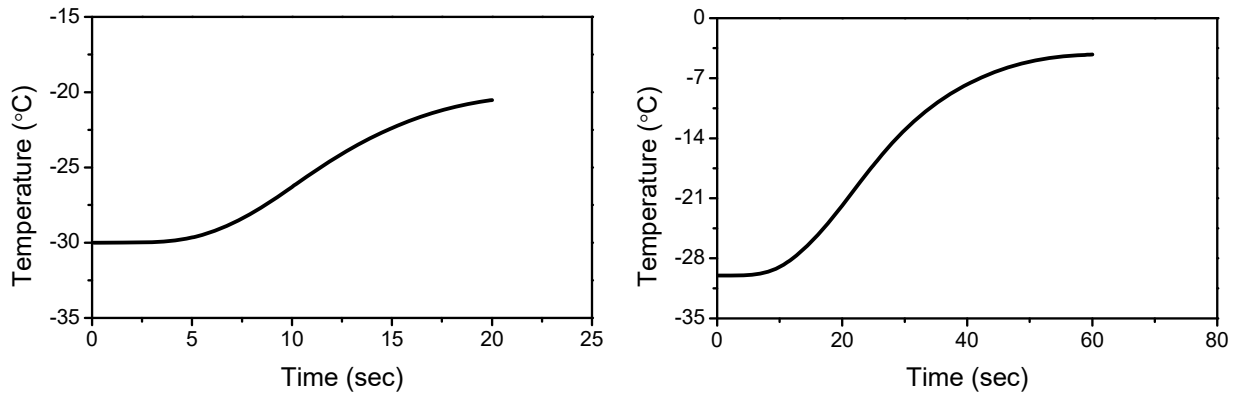**Figure 15**   Tokachi-oki earthquake accelerations

(a) Under 20s Kobe earthquake   (b) Under 1 min. triple of Tokachi-Oki earthquake

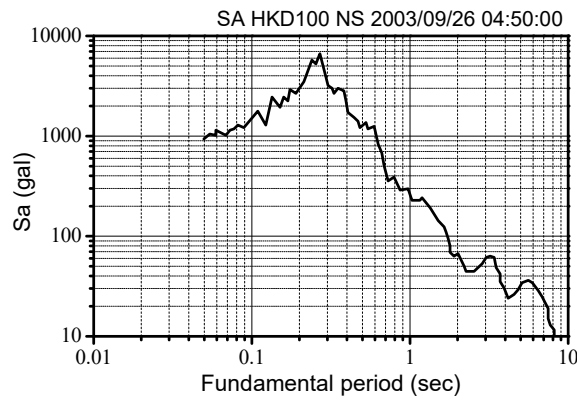**Figure 16**   Time histories of LRB-s-350 from thermal analysis

SA HKD100 NS 2003/09/26 04:50:00

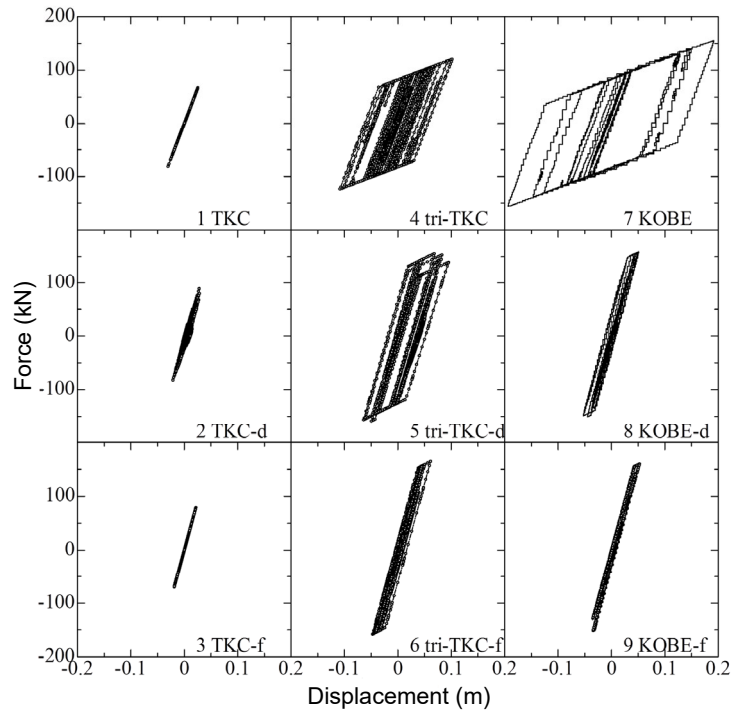**Figure 17**   Response spectrum of Tokachi-oki Earthquake, *L* (*NS*)

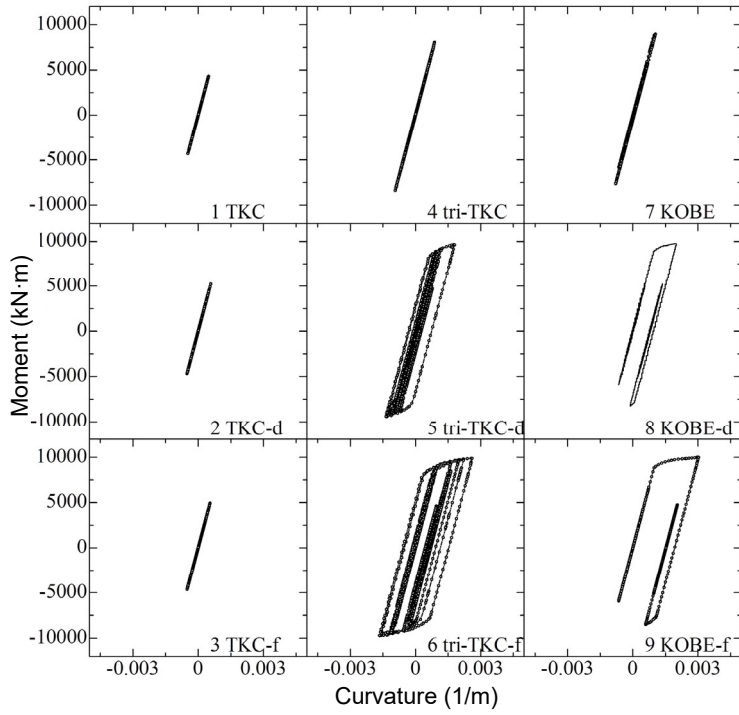**Figure 18**   Shear force-displacement response at bearing (P3 *X*-direction)

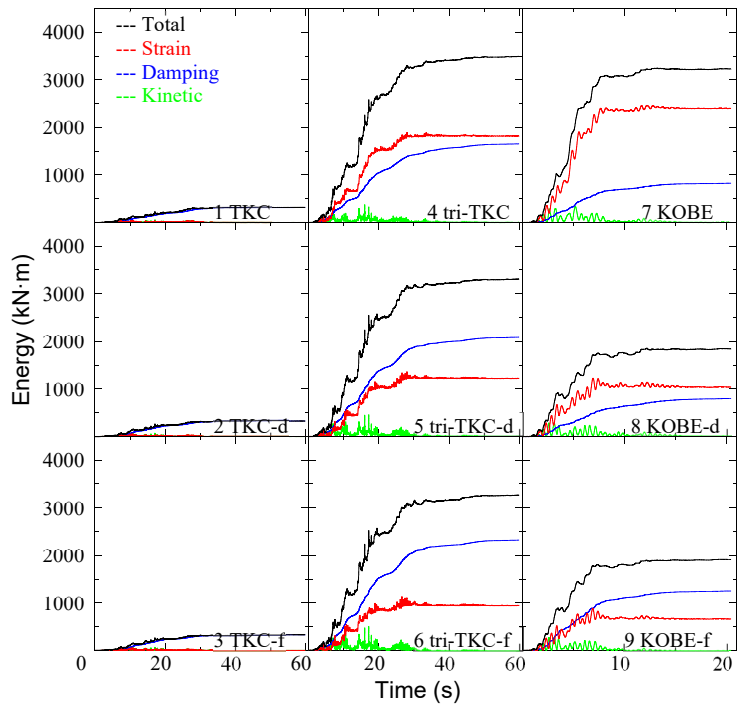**Figure 19**   Bending moment-curvature response (P3 *X*-direction)

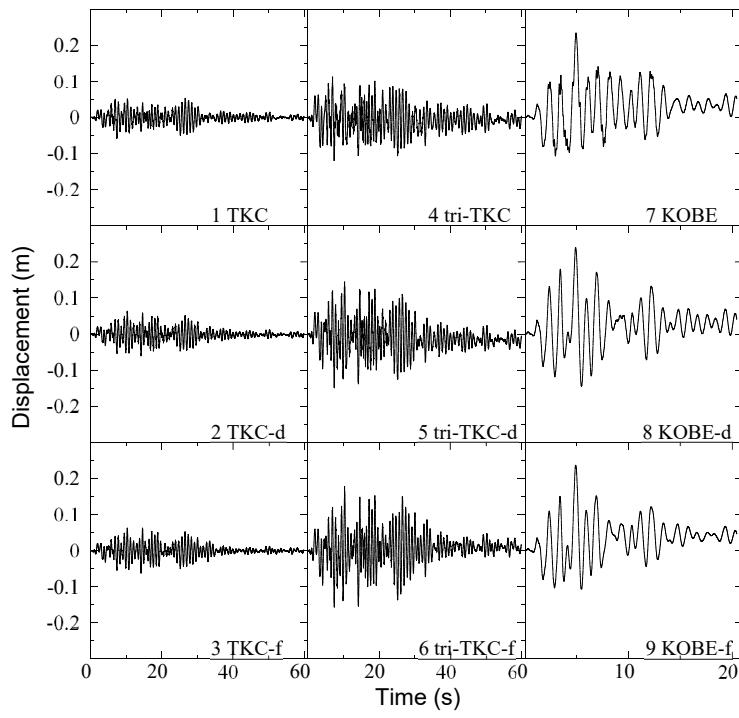**Figure 20**   Energy time history

1

Figure 21   Displacement time history at the tops of piers (P3 *X*-direction)

2
3
4
5

TABLES

Table 1 Geometry and material properties of LRB

Geometry parameter				(Rubber layer thickness t_r = 8 mm)
L (mm)	200	350	500	Rubber square side length
T_e (mm)	112	136	160	Total rubber height
H_b (mm)	234	280	326	Total isolator's height
Rubber material property				(Rubber code: G4)
G (N/mm^2)	0.385			Shear modulus
E_B (N/mm^2)	1176			Bulk modulus of elasticity
E_0 (N/mm^2)	2.20			Young's modulus of rubber
κ	0.85			Young's modulus correction factor according to hardness
Steel and lead plug				
Reinforced steel plate				SS400（JIS G 3101）
Flange plate				SS400（JIS G 3101）
Connecting plate				SS400（JIS G 3101）
Lead plug				Pb（JIS H 2105 special）

Table 2 Structural properties of bearing (K(MN/m), F(MN))

LRB product	Side length (mm)	K_1 (MN/m)	K_2 (MN/m)	K_3 (MN/m)	F_1 (MN)	F_2 (MN)
LRB-S-200	200	1.489	0.212	0.549	0.063	0.125
LRB-S-350	350	2.662	0.380	0.984	0.096	0.191
LRB-S-500	500	3.850	0.550	1.425	0.138	0.275

Table 3 Fundamental Natural Frequencies and Periods

No. of cases	Name of cases	ω [rad/sec]	T [sec]	Ratio to T at case 10	Support conditions Bearings	Temperature
1	s200	3.53	1.78	2.07	LRB-S-200	+20°C&No variation
2	s200l-d	3.72	1.70	1.97	LRB-S-200	-30°C&Include variation
3	s200l-f	3.91	1.61	1.87	LRB-S-200	-30°C&No variation
4	s350	4.38	1.44	1.67	LRB-S-350	+20°C&No variation
5	s350l-d	4.58	1.38	1.60	LRB-S-350	-30°C&Include variation
6	s350l-f	4.77	1.32	1.53	LRB-S-350	-30°C&No variation
7	s500	4.94	1.27	1.48	LRB-S-500	+20°C&No variation
8	s500l-d	5.13	1.23	1.42	LRB-S-500	-30°C&Include variation
9	s500l-f	5.32	1.18	1.37	LRB-S-500	-30°C&No variation
10	fixed	7.340	0.856	1.00	Fixed	+20°C&No variation

Table 4 Fundamental Natural Frequencies

No. of cases	Earthquake	Temperature	ω[rad/sec]	T[sec]	ratio to T of fix
1	Tokachi	+20℃&No variation	4.38	1.44	1.67
2	Tokachi	-30℃&Include variation	4.58	1.38	1.60
3	Tokachi	-30℃&No variation	4.77	1.32	1.53
4	Tokachi-triple	+20℃&No variation	4.38	1.44	1.67
5	Tokachi-triple	-30℃&Include variation	4.58	1.38	1.60
6	Tokachi-triple	-30℃&No variation	4.77	1.32	1.53
7	Kobe	+20℃&No variation	4.38	1.44	1.67
8	Kobe	-30℃&Include variation	4.58	1.38	1.60
9	Kobe	-30℃&No variation	4.77	1.32	1.53
10	--	+20℃&No variation	7.34	0.86	1